TiO$_2$-assisted GaN-nanowire-based stable ultraviolet photoelectrochemical detection

Yang Kang[*], Xin Liu[*], Danhao Wang, Shi Fang, Yuanmin Luo, and Haiding Sun [✉]

School of Microelectronics, University of Science and Technology of China, Hefei 230029, China

* These authors contributed equally to this work
✉Correspondence: Haiding Sun, E-mail: haiding@ustc.edu.cn

Graphical abstract

Ultrathin TiO$_2$ protecting layer improves the photostability of GaN-nanowire-based photoelectrochemical ultraviolet photodetectors.

Public summary

■ Using the atomic layer deposition technique, a thickness of 4 nm TiO$_2$ protective layer was deposited on the GaN nanowires.

■ The ultrathin TiO$_2$ protective layer can protect the GaN segment from corrosion and oxidation.

■ The photocurrent-attenuation coefficient of the coated GaN nanowires can be alleviated to 49%, while this number is as high as 85% in those uncoated GaN nanowires.

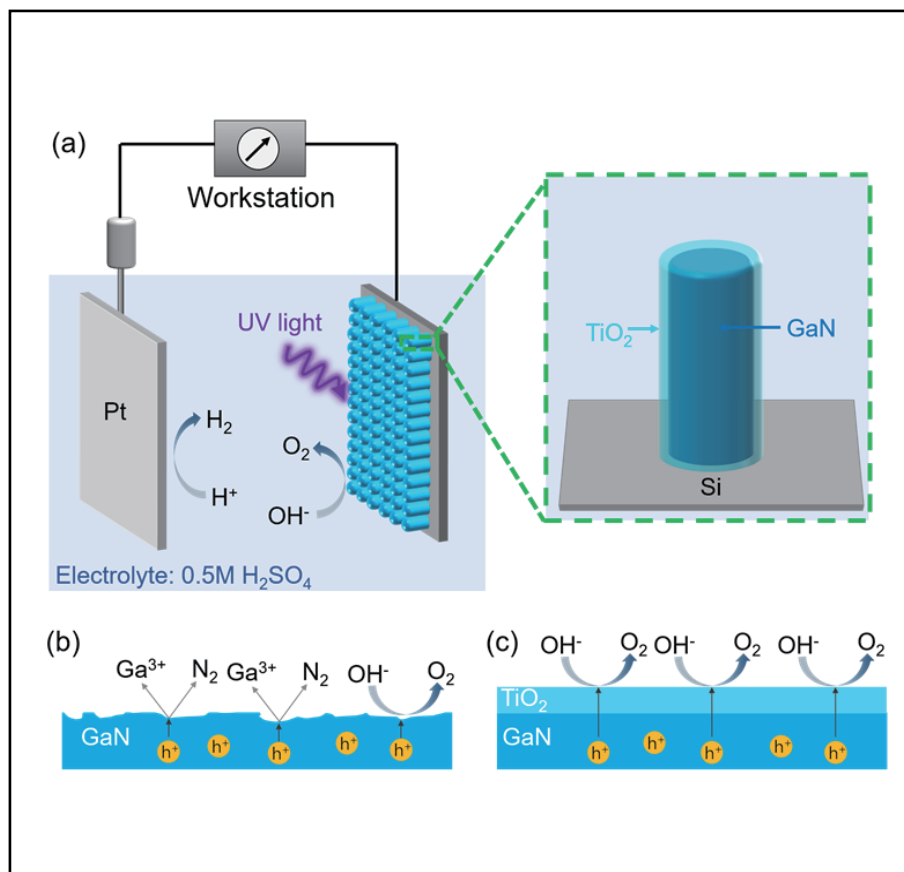# TiO₂-assisted GaN-nanowire-based stable ultraviolet photoelectrochemical detection

Yang Kang*, Xin Liu*, Danhao Wang, Shi Fang, Yuanmin Luo, and Haiding Sun ✉

School of Microelectronics, University of Science and Technology of China, Hefei 230029, China

* These authors contributed equally to this work
✉Correspondence: Haiding Sun, E-mail: haiding@ustc.edu.cn

Abstract: Ultraviolet photodetection plays an important role in optical communication and chemical- and bio- related sensing applications. Gallium nitride (GaN) nanowires-based photoelectrochemical-type photodetectors, which operate particularly in acqueous conditions, have been attracted extensive interest because of their low cost, fast photoresponse, and excellent responsivity. However, GaN nanowires, which have a large surface-to-volume ratio, suffer suffered from instability in photoelectrochemical environments because of photocorrosion. In this study, the structural and photoelectrochemical properties of GaN nanowires with improved photoresponse and chemical stability obtained by coating the nanowire surface with an ultrathin TiO₂ protective layer were investigated. The photocurrent density of TiO₂-coated GaN nanowires changed minimally over a relatively long operation time of 2000 s under 365-nm illumination. Meanwhile, the attenuation coefficient of the photocurrent density could be reduced to 49%, whereas it is as high as 85% in uncoated GaN nanowires. Furthermore, the photoelectrochemical behavior of the nanowires was investigated through electrochemical impedance spectroscopy measurements. The results shed light on the construction of long-term-stable GaN-nanowire-based photoelectrochemical-type photodetectors.

Keywords: GaN nanowires; photoelectrochemical-type photodetectors; TiO₂ protective layer; chemical stability

CLC number: TN29   **Document code:** A

1 Introduction

Photodetectors, which can convert absorbed optical signals into measurable electrical signals, are of central importance in modern optoelectronics[1]. Ultraviolent optical detection has been widely used in remote invisible light sensing, environmental monitoring, flame detection, chemical- and bio-sensors, and secure space-to-space communication. To achieve such practical applications, various ultraviolet (UV) photodetectors (PDs), include P–N junctions[2], photoconductances[3], Schottky junctions[4], and metal–semiconductor–metal based structures[5], have been reported in recent decades. Compared with conventional solid-state photodetectors, photoelectrochemical cell (PEC) PDs are highly desirable because of their unique operation in an aqueous environment for bio-related sensor applications[6]. Recently, group III nitride semiconductors have been regarded as promising candidates for developing PEC UV-PDs because of their high absorption coefficient, large charge carrier mobility, and tunable band energy bandgaps, which span the entire UV spectrum[7, 8]. However, GaN nanowires suffer from severe photocurrent attenuation caused by photocorrosion in acidic or alkaline electrolytes[9]. Therefore, it is critical to resolve the stability issue to achieve high-performance GaN-nanowire-based PEC UV-PDs.

CoOₓ nanoislands have been recently investigated to improve the photostability of the GaN nanowire photoanodes[10]. However, the nanoislands result in incomplete coverage over the surface of the nanowires, which leads to limited photostability in the strongly acidic or alkaline electrolytes. Photocorrosion protection requires the protective layer to be pinhole free and conformal—qualities that are difficult to obtain using solution or physical vapor-based deposition methods[11]. Fortunately, metallic oxide layers synthesized by atomic layer deposition (ALD) can provide continuous, conformal films with thickness in the nanometer scale, thereby inhibiting the photocorrosion of the nanostructures[12]. For instance, TiO₂ deposited by ALD has been demonstrated to be an excellent corrosion-resistant layer for protecting nanostructures from photocorrosion while making the tunneling of electrons or holes to the electrolyte possible[13].

In this study, it was found that the photostability of GaN nanowire-based PEC UV-PDs can be significantly improved by depositing an ultrathin TiO₂ protecting layer on the nanowire surface. A 4-nm-thick TiO₂ protective layer was successfully deposited on GaN nanowires using ALD. The TiO₂-coated GaN (GaN@TiO₂) operated stably for 2000 s under 365 nm illumination, and the system become more stable than the nanowires without coating. Simultaneously, the photocurrent density attenuation coefficient of the GaN nanowires decreased from 85% to 49% after TiO₂ deposition. The suppression of photocorrosion of the GaN@TiO₂ nanowires was investigated, as well as the charge transfer efficiency, using electrochemical impedance spectroscopy (EIS). It was demonstrated that ultrathin corrosion-resistant materials, such as TiO₂, can be applied to construct stable GaN nanowire-based photoelectrochemical-type photodetectors.

2 Results and discussion

2.1 Structure and morphologic characterizations

In this study, n-type GaN nanowires were grown on Si (111) substrates by molecular beam epitaxy (MBE). Ultrathin overlayers of TiO$_2$ were directly deposited on the surface of the GaN nanowires using ALD. As schematically displayed in Fig. 1 a, a complete ALD cycle includes four steps. First, tetrakis dimethylamino titanium (TDMAT) was adsorbed onto the surface of the GaN nanowires; the excess gases were purged by N$_2$. Then, H$_2$O entered the chamber and reacted with TDMAT. Finally, excess H$_2$O and by-products were purged with N$_2$. Transmission electron microscopy (TEM) of individual GaN@TiO$_2$ nanowires, as shown in Fig. 1 b and c, clearly revealed the core–shell structure of the nanowires. Typically, the diameter of the nanowire is approximately 80 nm, and the thickness of the TiO$_2$ layer is approximately 4 nm. The elemental distribution in the nanowires was analyzed using scanning transmission electron microscopy (STEM) energy-dispersive X-ray spectroscopy (EDS) measurement. The variation of the Ga, N, Ti, and O signals perpendicular to the nanowire axial direction (green line in high-angle annular dark-field image) is shown in Fig. 1 d and e. The EDS analysis demonstrates the uniform coverage of the GaN nanowire by the TiO$_2$ layer, as shown in Fig. 1 e. However, the TiO$_2$ layer is indistinguishable in scanning electron microscopy (SEM) image because of its ultrathin thickness (approximately 4 nm), as shown in Fig. 1 f.

2.2 PEC measurements

Fig. 2 shows a schematic illustration of the photodetection characteristics of the PEC UV-PDs. First, as-grown GaN nanowires and GaN@TiO$_2$ nanowires were employed to fabricate the photoelectrodes. In theory, when N-type GaN nanowires or GaN@TiO$_2$ nanowires are in contact with the electrolyte, the nanowires exhibit an upward band bending at the nanowire–electrolyte interface owing to the establishment of electrochemical equilibrium[14]. When the GaN nanowires are illuminated by UV photons, with upward band bending as the driving force, the photogenerated holes (h$^+$) are more likely to drift to the GaN nanowire–electrolyte interface and participate in the redox reaction: $2H_2O + 4h^+ = O_2 + 4H^+$. Meanwhile, the upward band bending induces the directional transfer of electrons (e$^-$) in the opposite direction, which is toward the Pt counter electrode, undergoing reduction reaction: $4H^+ + 4e^- = 2H_2$, completing the current loop[7]. The electrical signals in the current loop can be collected and recorded by the electrochemical workstation.

Ideally, all the h$^+$ should be consumed by the redox reaction with H$_2$O. However, in PEC environments, some of the photogenerated charge carriers participate in the self-oxidation of semiconductors, called "photocorrosion". Notably, n-type GaN nanowires can be easily oxidized by photoexcited h$^+$, participating in the redox reaction: $2GaN + 6h^+ = 2Ga^{3+} + N_2$[15], as displayed in Fig. 2 b. As a result of this redox reaction, the damage to nanowire surface decreases the photoresponse ability because of the photocorrosoin of the GaN nanowires. However, the stability of the GaN-nanowire-based photoelectrode is an important consideration for the practical use of the PEC UV-PDs. The ultrathin TiO$_2$ layer is expected to build up a physical separation of the GaN nanowires from the electrolyte, while allowing tunneling of the photogenerated carriers from the GaN nanowires to the electrolyte, which contributes to the photocurrent, as illus-
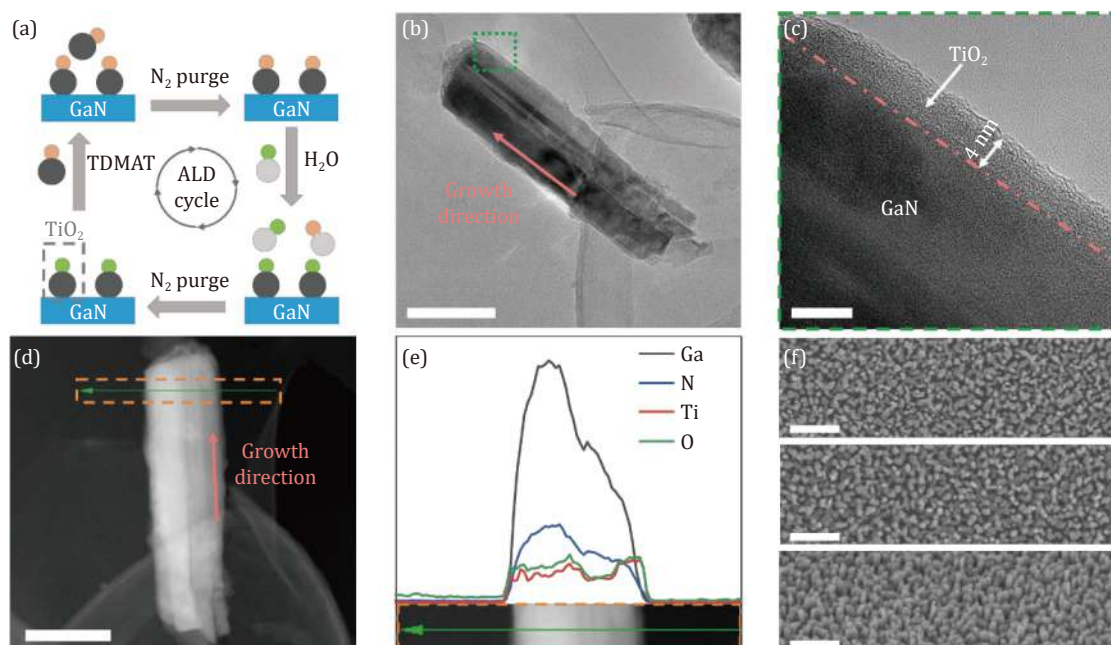

Fig. 1. (a) Schematic illustration of ALD decoration process. (b) Overview of the TEM image of GaN@TiO$_2$ nanowire (scale bar, 100 nm). (c) Selected-area TEM image of GaN@TiO$_2$ nanowire (scale bar, 10 nm). (d) STEM image of GaN@TiO$_2$ nanowire (scale bar, 100 nm). (e) EDS line profiles of Ga, N, Ti, and O across the GaN@TiO$_2$ nanowire. (f) Top-view SEM images of GaN nanowires (top; scale bar, 500 nm) and GaN@TiO$_2$ nanowires (middle; scale bar, 500 nm), and side-view SEM image of GaN@TiO$_2$ nanowires (bottom; scale bar, 500 nm).
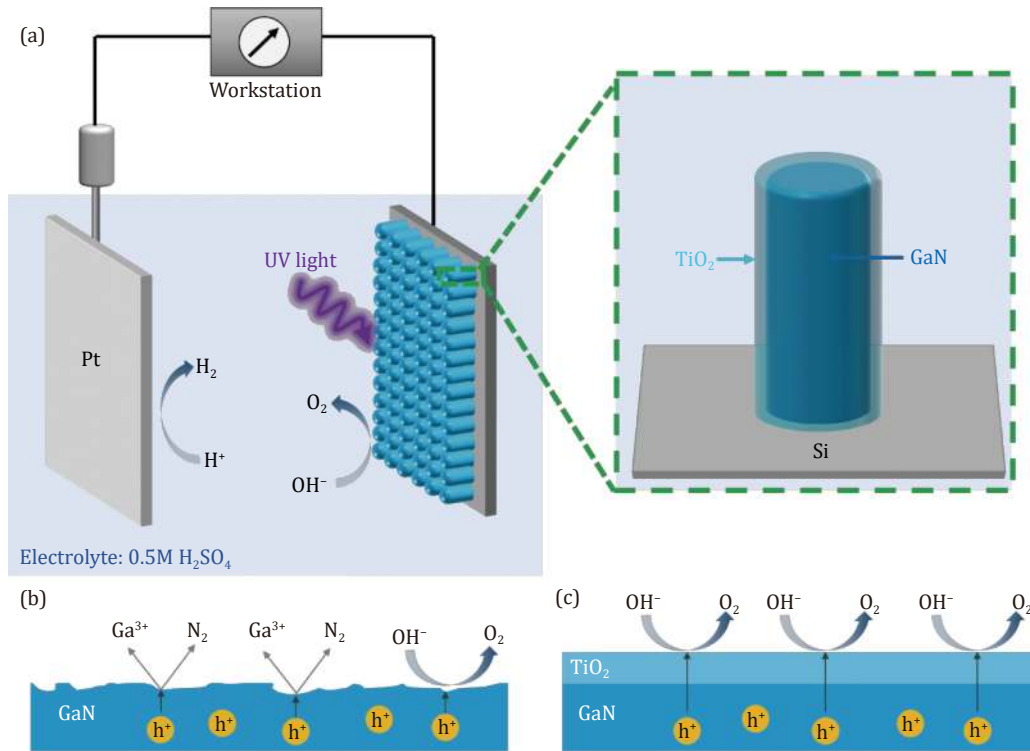
Fig. 2. (a) Schematic illustration of the operation of the GaN@TiO$_2$-nanowire-based PEC UV-PDs under UV light irradiation. (b) Bare GaN nanowire surface in which photocorrosion predominates. (c) GaN coated with TiO$_2$ layer, where photogenerated holes can oxidize OH$^-$ to O$_2$.

trated in Fig. 2 c

To characterize the photocurrent stability of the GaN nanowires and the GaN@TiO$_2$ nanowires, the photocurrent density J_{photo} is defined as[6]

$$J_{photo} = J_{light} - J_{dark} \qquad (1)$$

where J_{light} and J_{dark} are the current density with and without light, respectively.

The photocurrent density attenuation coefficient is defined as

$$\alpha = \frac{J_{photo-first} - J_{photo-last}}{J_{photo-first}} \times 100\% \qquad (2)$$

where $J_{photo-first}$ and $J_{photo-last}$ are the photocurrent densities when the light is turned on at the very beginning and before the light is turned off, respectively. Fig. 3 shows the typical photocurrent density as a function of time ($J–t$) data obtained under 365 nm illumination for bare GaN nanowires as well as for GaN@TiO$_2$ nanowires in 0.5 mol/L H$_2$SO$_4$ (aq) (pH=1). The J_{photo} of the bare GaN-nanowire-based PEC UV-PDs sharply decreased over 250 s because of severe photocorrosion. By contrast, the GaN@TiO$_2$-nanowire-based PEC UV-PDs showed little change in J_{photo} over 2000 s. Meanwhile, the photocurrent density attenuation coefficient α decreased from 85% for GaN nanowires to 49% for GaN@TiO$_2$ nanowires, which clearly demonstrates the effectiveness of the TiO$_2$ protective layer, which can inhibit photocorrosion of the GaN nanowires.

After 2000 s of illumination, the photocurrent of both the GaN nanowire and GaN@TiO$_2$ nanowire PEC UV-PDs tended to be stable. The response and recovery characteristics of the devices were measured after stabilization. The response time (t_{res}) is the time required for the photocurrent to increase from 10% to 90% of the maximum value, whereas the recovery time is the time required for the photocurrent to decrease from 90% to 10%. As indicated in Fig. 3 b and c, the response speed of both GaN nanowire and GaN@TiO$_2$ nanowire PEC UV-PDs are in the order of milliseconds, verifying the rapid photoresponse of the devices. Another critical index responsivity (R), was calculated using the equation

$$R = J_{photo}/P_{light} \qquad (3)$$

where P_{light} is defined as the light intensity. The responsivity of the GaN@TiO$_2$ nanowires improved compared with that of the GaN nanowires after 2000 s of illumination, as shown in Fig. 3 b and c. However, the $J_{photo-first}$ of the GaN nanowires decreased after coating with the TiO$_2$ protective layer. This may be because the TiO$_2$ protective layer suppresses the charge transfer at the nanowires-electrolyte interface, as discussed later.

To investigate further the photocorrosion suppression and charge transfer efficiency after using the TiO$_2$ protective layer, in-depth electrochemical investigations of the GaN and GaN@TiO$_2$ nanowires were carried out using EIS under 365 nm illumination. The EIS measurements were performed over a frequency range of 10^6~0.1 Hz and at an amplitude of 5 mV. Thereafter, as shown in Fig. 4, the EIS results were fitted using an equivalent circuit R_Ω (R_1–CPE$_1$) (R_2–CPE$_2$), in which R_Ω is the ohmic resistance caused by the electrolyte; CPE$_1$ and CPE$_2$ are constant phase elements, and R_1, R_2 represent polarization resistance[16,17]. The simulated data of the experi-
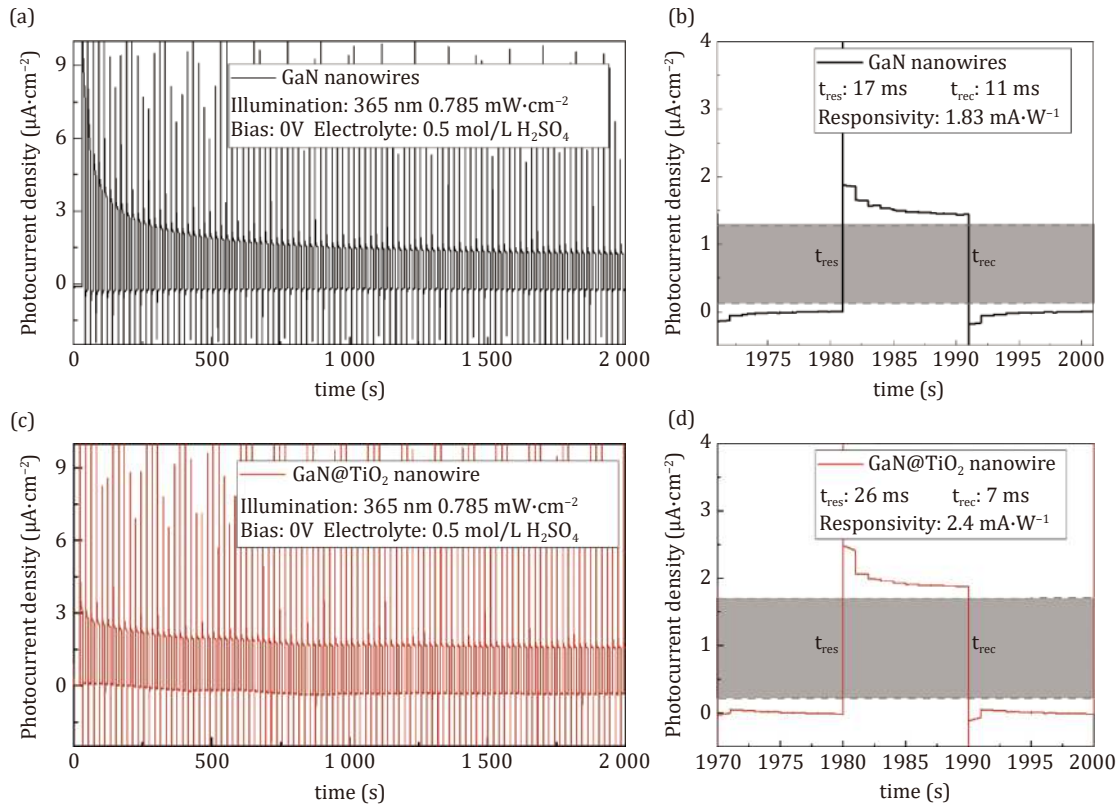
Fig. 3. (a) *J-t* characteristics of GaN-nanowire-based PEC UV-PDs under 365 nm irradiation. (b) Representation of the rise time and decay time interval of GaN-nanowire-based PEC UV-PDs. (c) GaN@TiO$_2$-nanowire-based PEC UV-PDs under 365 nm irradiation. (d) Representation of the rise time and decay time interval of GaN@TiO$_2$-nanowire-based PEC UV-PDs.

mental results using ZView software are summarized in Table 1.

As shown in Table 1, EIS analysis reveals a significant difference in the polarization resistance at the nanowire–electrolyte interface in the GaN nanowires with and without the TiO$_2$

layer. Specifically, the total polarization resistance R_p is

$$R_p = R_1 + R_2 \qquad (4)$$

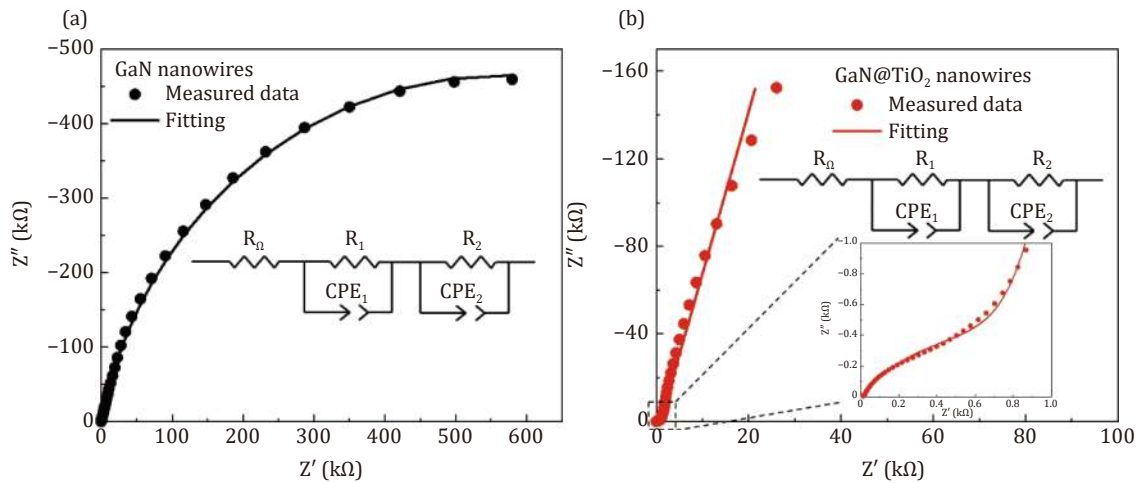As a result, the R_p of the GaN@TiO$_2$ nanowires is much

Fig. 4. Photoelectrochemical impedance spectra of (a) GaN-nanowire-based and (b) GaN@TiO$_2$-nanowire-based PEC UV-PDs under 365 nm irradiation.

Table 1. EIS fitted data using ZView software, where R and CPE are in Ω cm^2 and Yo [$(S\text{-}s)^n$ cm^{-2}], respectively.

Nanowire	R_Ω	R_1	CPE$_1$	n	R_2	CPE$_2$	n
GaN	13.09	4.8×10^5	3.1×10^{-6}	0.88	6.5×10^5	2.3×10^{-6}	0.88
GaN@TiO$_2$	9.56	836	7.4×10^{-6}	0.69	1.0×10^{20}	1.0×10^{-6}	0.91

higher than that of the uncoated GaN nanowires, indicating that the TiO_2 coated on GaN nanowires has a high electrical insulating property. Hence, anodic oxidation on the surface of the coating rarely occurs. Therefore, the value of R_p is directly related to the efficiency of photocorrosion inhibition. To further compare the photocorrosion inhibition efficiency of the uncoated GaN nanowires and GaN@TiO_2 nanowires, the photocorrosion inhibition enhancement factor is defined as

$$\beta = (R_{pALD} - R_{pbare})/R_{pALD} \tag{5}$$

where R_{pbare} and R_{pALD} are the polarization resistances of the GaN and GaN@TiO_2 nanowires, respectively. The calculated value of β obtained from the measured data is almost equal to unity, which demonstrates a significant enhancement in the photocorrosion inhibition of GaN nanowires by the TiO_2 coating[18]. Meanwhile, the polarization resistance is related to the charge transfer efficiency at the nanowire–electrolyte interface[19]. The higher polarization resistance at the interface between the nanowires and the electrolyte may lead to a lower charge transfer efficiency, which can be responsible for the limited photocurrent density of the GaN@TiO_2 nanowires.

3   Experimental

3.1   MBE growth of GaN nanowires

The *n*-type GaN nanowires were grown on planar Si (111) substrates using plasma-assisted MBE (PAMBE) under nitrogen-rich conditions. Before the Si (111) substrate was loaded into the PAMBE chamber, the surface oxide on the substrate was removed by the BOE(buffered oxide etching) solution. Then, the Si (111) substrate was outgassed in the load-lock chamber at 200 °C for 1 h to eliminate the organic-based contaminants and water components. For the N-type GaN nanowire growth, nitrogen was supplied by the radio frequency plasmon source, and the controlled Ga and Si fluxes were used by the thermal effusion cells.

3.2   ALD growth of TiO_2 layer

TiO_2-deposition was performed on the as-grown GaN nanowires in a customized flow-type ALD reactor (Oxford Instruments-FlexAl). The precursors used for TiO_2 were TDMAT as the titanium source and H_2O as the oxygen source. The titanium source was sublimated at 90 °C. H_2O was then evaporated at 20 °C. The substrate temperature was maintained at 250 °C. The optimized deposition conditions produced 0.6 Å of TiO_2-growth for each cycle. One cycle of the TiO_2-ALD consists of four steps: ① Titanium metal source feeding (20 sccm) for 0.2 s; ② Purging for 6 s, ③ H_2O feeding (40 sccm) for 0.1 s; ④ Purging for 8 s. Nitrogen was used as purging and carrier gas. Seventy-two cycles were performed on the GaN nanowires.

3.3   Characterization methods

The detailed morphology of the nanowires was determined using TEM, STEM, and EDS measurements, which were performed on a Tools F200X instrument.

3.4   Fabrication of photoelectrode

The GaN nanowires/Si wafers and GaN@TiO_2 nanowires/Si wafers were cut to the desired size. First, the surface oxide on the back of the Si wafer was removed. Then, a Ga–In eutectic alloy (Alfa Aesar) was deposited on the back of the Si wafer to form an ohmic contact. The wafer was then mounted onto a copper sheet with a silver paste. Except for the nanowire surface that contacted the electrolyte, the entire wafer was then covered with insulating epoxy to avoid leakage current. Before measurement, the epoxy was dried in air for 24 h.

3.5   PEC measurement

The typical photocurrent performance and EIS analysis was performed using a CHI 760E electrochemical workstation with a standard three-electrode system. The three-electrode system was constructed in quartz reaction cell (CEL-CPE50) with a high UV transmittance. The as-prepared nanowire electrode, Ag/AgCl (saturated KCl), and platinum nets served as the working electrode, respectively. An aqueous solution of H_2SO_4 (0.5 mol/L) was chosen as the electrolyte. A light-emitting diode was chosen as electrolyte. A LED was used to generate 365 nm light to irradiate the nanowires. The light intensity was fixed at 0.785 mW cm^{-2}, which was calibrated using an optical power meter (S401C and PM100D). A shutter was used to switch the light on and off. The time for turning on and turning off the light was set at 10 s. The potentiostatic EIS measurement was performed using a DC signal of a magnitude 5 mV at a frequency range of 0.1~10^6 Hz with 365 nm illumination. ZView software was used to fit the measured EIS data.

4   Conclusions

In this study, the experimental results demonstrated that the photoelectrochemical stability of GaN nanowires can be significantly enhanced by coating with an ultrathin TiO_2 film using ALD. The TiO_2-coated GaN nanowires showed a reduced photocurrent density attenuation coefficient of 49% under 365 nm illumination, whereas untreated GaN nanowires exhibited a high value of 85%. Thus, the ultrathin coating successfully protected the GaN nanowires against photocorrosion. However, the photocurrent density of the GaN nanowires decreased after they were coated with TiO_2, mainly because of the lower charge transfer efficiency, according to the EIS analysis. Adopting novel protective layers or active sites to provide improved stability and photoresponse performance is planned in future endeavors.

Author contributions

Haiding Sun conceived the study and designed the experiments. Xin Liu, Yang Kang, Danhao Wang, and Yuanmin Luo fabricated the devices. Xin Liu, Yang Kang, and Shi Fang performed the optical characterization and photoelectro-

chemical experiments. Yang Kang, Xin Liu, Danhao Wang, and Haiding Sun wrote the initial manuscript, which was revised by other co-authors. All authors approved the final version of the manuscript.

Conflict of interest

The authors declare that they have no conflict of interest.

Biographies

Yang Kang   is currently pursuing his Master Degree in School of Microelectronics at University of Science and Technology of China. His primary research is related with optoelectronic materials and devices. He has published first author papers including IEEE Transation on Electronic Devices, ACS Applied Nano Materials, etc.

Xin Liu(co-first author)   is currently pursuing his Master Degree in School of Microelectronics at University of Science and Technology of China. His primary research is related with optoelectronic materials and devices. He has published first author papers including Advanced Functional Materials etc.

Haiding Sun   received his Ph.D. in Electrical Engineering from Boston University. He is currently a Professor in the School of Microelectronics at University of Science and Technology of China. He has published more than 90+ peer-reviewed SCI-index journal papers including Nature Electronics, Advanced Functional Materials, Nano Letters, IEEE Electron Device Letters, Applied Physics Letters etc. His research interests include the investigation of the physics, MBE and MOCVD epitaxy, fabrication, and characterization of wide bandgap semiconductor materials for both optoelectronics and electronic devices. His work has been highlighted by more than 100 times in many media outlets including Compound Semiconductors, Semiconductors Today, Phys.org, Nanowerk etc. He is an IEEE Senior Member. He is currently Associated Editor of *IEEE Photonics Technology Letters*, *SPIE Journal of Nanophotonics*, *ASME Open Journal of Engineering*, and Guest Editor of *Journal of Electronic Packaging* and *Crystal*.

References

[1] Mauthe S, Baumgartner Y, Sousa M, et al. High-speed III-V nanowire photodetector monolithically integrated on Si. *Nat. Commun.,* **2020**, *11* (1): 4565.

[2] Wang Y, Wu C, Guo D, et al. All-oxide NiO/Ga_2O_3 P–N junction for self-powered UV photodetector. *ACS Appl. Electron. Mater.,* **2020**, *2* (7): 2032–2038.

[3] Gao Y, Lei S, Kang T, et al. Bias-switchable negative and positive photoconductivity in 2D $FePS_3$ ultraviolet photodetectors. *Nanotechnology,* **2018**, *29* (24): 244001.

[4] Zhang T F, Wu G A, Wang J Z, el al. A sensitive ultraviolet light photodiode based on graphene-on-zinc oxide Schottky junction. *Nanophotonics,* **2016**, *6* (5): 1073–1081.

[5] An Q, Meng X, Xiong K, et al. Self-powered ZnS nanotubes/Ag nanowires MSM UV photodetector with high On/Off Ratio and fast response speed. *Sci. Rep.,* **2017**, *7* (1): 4885.

[6] Wang D, Liu X, Fang S, et al. Pt/AlGaN nanoarchitecture: Toward High Responsivity, Self-Powered Ultraviolet-Sensitive Photodetection. *Nano Lett.,* **2021**, *21* (1): 120–129.

[7] Wang D, Huang C, Liu X, et al. Highly uniform, self‐assembled AlGaN nanowires for self‐powered solar‐blind photodetector with fast‐response speed and high responsivity. *Adv. Opt. Mater.,* **2020**, *9* (4): 2000893.

[8] Fang S, Wang D, Wang X, et al. Tuning the charge transfer dynamics of the nanostructured GaN photoelectrodes for efficient photoelectrochemical detection in the ultraviolet band. *Adv. Funct. Mater.,* **2021**, *31* (29): 2103007.

[9] Wang Q, Yuan G, Zhao S, et al. Metal-assisted photochemical etching of GaN nanowires: The role of metal distribution. *Electrochem. Commun.,* **2019**, *103*: 66–71.

[10] Liu G, Karuturi S K, Simonov A N, et al. Robust Sub‐monolayers of Co_3O_4 nano‐islands: A highly transparent morphology for efficient water oxidation catalysis. *Adv. Energy Mater.,* **2016**, *6* (15): 1600697.

[11] Steier L, Bellani S, Rojas H C, et al. Stabilizing organic photocathodes by low-temperature atomic layer deposition of TiO_2. *Sustain. Energy Fuels,* **2017**, *1* (9): 1915–1920.

[12] Chen Y W, Prange J D, Duhnen S, et al. Atomic layer-deposited tunnel oxide stabilizes silicon photoanodes for water oxidation. *Nat. Mater.,* **2011**, *10* (7): 539–544.

[13] Hu S, Shaner M R, Beardslee J A, et al. Amorphous TiO_2 coatings stabilize Si, GaAs, and GaP photoanodes for efficient water oxidation. *Science,* **2014**, *344* (6187): 1005–1009.

[14] Hisatomi T, Kubota J, Domen K. Recent advances in semiconductors for photocatalytic and photoelectrochemical water splitting. *Chem. Soc. Rev.,* **2014**, *43* (22): 7520–7535.

[15] Ohkawa K, Ohara W, Uchida D, et al. Highly stable GaN photocatalyst for producing H_2 gas from water. *JPN. J. Appl. Phys.,* **2013**, *52* (8S): 08JH04.

[16] Park K, Zhang Q, Garcia B B, et al. Effect of an ultrathin TiO_2 layer coated on submicrometer-sized ZnO nanocrystallite aggregates by atomic layer deposition on the performance of dye-sensitized solar cells. *Adv. Mater.,* **2010**, *22* (21): 2329–2332.

[17] Mushtaq N, Xia C, Dong W, et al. Tuning the energy band structure at interfaces of the $SrFe_{0.75}Ti_{0.25}O_3$-delta-$Sm_{0.25}Ce_{0.75}O_2$-delta heterostructure for fast Ionic transport. *ACS Appl. Mater. Inter,* **2019**, *11* (42): 38737–38745.

[18] Bahari H S, Savaloni H. Surface analysis of Cu coated with ALD Al_2O_3 and its corrosion protection enhancement in NaCl solution: EIS and polarization. *Mater. Res. Express,* **2019**, *6* (8): 086570.

[19] Yousaf M, Mushtaq N, Zhu B, et al. Electrochemical properties of $Ni_{0.4}Zn_{0.6}Fe_2O_4$ and the heterostructure composites (Ni–Zn ferrite-SDC) for low temperature solid oxide fuel cell (LT-SOFC). *Electrochimica Acta,* **2020**, *331*: 135349.